Testing the D/H ratio of alkenones and palmitic acid as salinity proxies in the Amazon Plume

C. Häggi[1], C. M. Chiessi[2] and E. Schefuß[1]

[1]{MARUM – Center for Marine Environmental Sciences, University of Bremen, Germany}

[2]{School of Arts, Sciences and Humanities, University of São Paulo, Brazil}

Correspondence to: C. Häggi (chaeggi@marum.de)

Abstract

The stable hydrogen isotope composition of lipid biomarkers, such as alkenones, is a promising new tool for the improvement of paleosalinity reconstructions. Laboratory studies confirmed the correlation between lipid biomarker δD composition (δD_{Lipid}), water δD composition (δD_{H_2O}) and salinity. Yet, there is limited insight into the applicability of this proxy in oceanic environments. To fill this gap, we test the use of the δD composition of alkenones (δD_{C37}) and palmitic acid (δD_{PA}) as salinity proxies using samples of surface suspended material along the distinct salinity gradient induced by the Amazon Plume. Our results indicate a positive correlation between salinity and δD_{H_2O}, while the relationship between δD_{H_2O} and δD_{Lipid} is more complex: δD_{PA} correlates strongly with δD_{H_2O} (r^2=0.81) and shows a salinity dependent isotopic fractionation factor. δD_{C37} only correlates with δD_{H_2O} in a small number (n=8) of samples with alkenone concentrations >10 ng L^{-1}, while there is no correlation if all samples are taken into account. These findings are mirrored by alkenone based temperature reconstructions, which are inaccurate for samples with low alkenone concentrations. Deviations in δD_{C37} and temperature are likely to be caused by limited haptophyte algae growth due to low salinity and light limitation imposed by the Amazon Plume. Our study confirms the applicability of δD_{Lipid} as a salinity proxy in oceanic environments. But it raises a note of caution concerning regions where low alkenone production can be expected due to low salinity and light limitation, for instance, under strong riverine discharge.

1 Introduction

The precise reconstruction of past ocean salinity is still a pending issue in paleoclimatology (Rohling, 2007). Until recently, most paleosalinity studies have relied on foraminifera based reconstructions of the stable oxygen isotope composition of seawater, which correlates with salinity (Epstein and Mayeda, 1953). However, temperature also controls the oxygen isotope composition of foraminifera, making corrections in the estimation of paleosalinity necessary (Lea et al., 2000;Rostek et al., 1993). The imprecision associated with this approach has led to the search for alternative salinity proxies. The use of the hydrogen isotopic composition of algal lipids (δD_{Lipid}) for the reconstruction of the stable hydrogen composition of water (δD_{H_2O}) is one of such recent developments (Sessions et al., 1999;Schouten et al., 2006). As outlined in a theoretical framework by Rohling (2007), this method has the potential to lead to more precise reconstructions of surface water salinity in combination with foraminifera based $\delta^{18}O$.

So far, efforts to apply δD_{Lipid} as a salinity proxy have mainly involved the use of long-chain alkenones. Long-chain alkenones have the advantage of being exclusively produced by specific haptophyte algae, and of showing good preservation over geologic timescales (Marlowe et al., 1984;Marlowe et al., 1990). Laboratory studies have confirmed the correlation of the D/H ratio of the C_{37} alkenones (δD_{C37}) with δD_{H_2O} (Englebrecht and Sachs, 2005;Schouten et al., 2006). Furthermore, the D/H fractionation factor between alkenones and water ($\alpha_{C_{37}}$)

$$\alpha_{C37} = \frac{\delta D_{C37} + 1000}{\delta D_{H_2O} + 1000} \quad (1)$$

was found to be salinity dependent, leading to a potentially twofold way to reconstruct salinity (Schouten et al., 2006). There are, however, potential factors that may compromise the use of δD_{C37} and $\alpha_{C_{37}}$ as salinity proxies. $\alpha_{C_{37}}$ is, for instance, inconsistent among different haptophyte algae species. Species preferring shelf environments have a higher $\alpha_{C_{37}}$ than species favoring open marine habitats (M'Boule et al., 2014). In some situations $\alpha_{C_{37}}$ has shown a small temperature dependency (Zhang and Sachs, 2007). Furthermore, $\alpha_{C_{37}}$ is also dependent on algal growth phase and rate (Schouten et al., 2006;Wolhowe et al., 2009;Chivall et al., 2014b). All these factors potentially exceed the effects of salinity and may impede the use of δD_{C37} as a paleosalinity proxy. Nevertheless, paleoclimate studies have made

successful use of δD_{C37} as a paleosalinity proxy (van der Meer et al., 2008;Giosan et al., 2012;Schmidt et al., 2014;Pahnke et al., 2007;van der Meer et al., 2007). However, in some cases, factors like species variability complicated δD_{C37} based salinity reconstructions (Kasper et al., 2015).

Apart from alkenones there is a variety of other algal lipids which feature a distinct δD_{H2O} – δD_{Lipid} relationship (Zhang et al., 2009;Sauer et al., 2001;Nelson and Sachs, 2014). Among these less frequently used compounds is palmitic acid. Palmitic acid is a saturated fatty acid, which is highly abundant in most aquatic environments. The infrequent use of palmitic acid is mainly due to its ubiquitous occurrence, which does not allow linkage to a single group of producing species. Furthermore, palmitic acid is less resistant to degradation than alkenones (Sun and Wakeham, 1994). Nevertheless, δD of palmitic acid (δD_{PA}) has been successfully used as a paleoclimate indicator in several studies (Huang et al., 2002;Smittenberg et al., 2011;Shuman et al., 2006).

Although there are numerous laboratory and paleoclimate studies confirming the applicability of δD_{Lipid} to reconstruct the past isotopic composition of water, there have been only few calibration studies in oceanic environments (Schwab and Sachs, 2011;Schwab and Sachs, 2009;Wolhowe et al., 2015). To fill this gap, we analyzed δD_{C37} and δD_{PA} of suspended particle samples along the salinity gradient induced by the Amazon freshwater plume and tested their applicability as salinity proxies (Fig. 1). Along with the hydrogen isotope analyses, we also tested the accuracy of the $U^{k'}_{37}$ temperature proxy (Müller et al., 1998) under the influence of the Amazon Plume. Potential impact of haptophyte species variability was monitored using the C_{37}/C_{38} ratio (Rosell-Mele et al., 1994), as defined below.

$$C_{37}/C_{38} = \frac{C_{37:3}Me + C_{37:2}Me}{C_{38:3}Et + C_{38:3}Me + C_{38:2}Et + C_{38:2}Me} \quad (2)$$

2 Methods

2.1 Study area

The study area is situated offshore northern Brazil and French Guyana close to the Amazon estuary (Fig 1). A large portion of the research area is influenced by freshwater outflow from the Amazon River, which induces a steep salinity gradient (Lentz and Limeburner, 1995). The freshwater plume is generally transported northwestwards by the North Brazil Current along

the coastline of northern Brazil and French Guyana, while areas to the southeast of the Amazon River Estuary are largely unaffected by the Amazon freshwater discharge (Geyer et al., 1996). The geometry and transport of the freshwater plume are subject to large seasonal variations. The plume reaches its maximum extent during peak Amazon discharge in boreal summer (Molleri et al., 2010), while its northwestward transport is controlled by wind-stress along the shelf (Geyer et al., 1996).

2.2 Sampling

Sampling was conducted during the RV *Maria S. Merian* cruise MSM20/3 from February 21th to March 9th 2012 (Mulitza et al., 2013). Samples of suspended particles were collected along a southeast to northwest transect off northeastern South America across the Amazon Plume (Fig. 1). Samples were taken via the ships seawater inlet at about 6 meters below sea level operated by a diaphragm pump. Between 100 and 500 litres of water were filtered over a period of 30 to 150 minutes on pre-combusted GFF filters. After sampling, filters were wrapped in pre-combusted aluminium foil and stored at -20°C. Along with the suspended particle samples, water samples were collected at the beginning and at the end of each filtering period. Water samples were sealed with wax and stored at 4°C before analysis. On-board salinity and temperature measurements were conducted in one second intervals by a SeaBird Electronics SBE 45 Micro thermosalinograph (accuracy 0.002°C and 0.005 psu).

2.3 Stable isotope analysis of water

The stable hydrogen isotope composition of seawater samples was determined at MARUM – Center for Marine Environmental Sciences, University of Bremen, with a Thermal-Conversion/Elemental-Analyser operated at 1400°C coupled to a ThermoFisher Scientific MAT 253 mass-spectrometer. Measurements were repeated ten times for each seawater sample. Four in-house water standards used for calibration were calibrated against IAEA standards VSMOW, GISP and SLAP. The maximum deviation from the calibration slope was 1.6 ‰ vs. VSMOW and the average deviation was 0.7 ‰ vs. VSMOW.

2.4 Lipid analysis

Suspended particle samples were freeze-dried in a Christ Alpha 1-4 freeze-dryer. Lipids were extracted in a DIONEX Accelerated Solvent Extractor (ASE 200) using a dichloromethane

(DCM): methanol (MeOH) 9 : 1 solution at 1000 psi and 100 °C for three cycles lasting 5 minutes each. Prior to extraction 2-Nonadecanone and erucic acid were added as internal standards for the ketone and acid fractions, respectively. After extraction, samples were dried in a Heidolph ROTOVAP system. The extracts were saponified using 0.1 M KOH in MeOH, yielding neutral and acid fractions. The neutral fraction was separated in three fractions using activated silica gel chromatography (1% H_2O). The first fraction was eluted with hexane, yielding saturated and unsaturated hydrocarbons. The second fraction was eluted with (DCM), yielding ketones, including alkenones. The third fraction was eluted with DCM:MeOH 1:1, yielding polar compounds. The acid fraction was methylized with MeOH of known isotopic composition (-156 ± 2 ‰ vs. VSMOW), yielding the corresponding fatty acid methyl esters (FAMEs). The FAMEs were subsequently cleaned over pipet columns containing two centimeters of silica. In order to remove unsaturated compounds, further cleaning over columns of two centimeters of $AgNO_3$ was conducted. Ketones and FAMEs were analyzed using a ThermoFisher Scientific Focus gas chromatograph equipped with an Rxi-5ms 30x column (30 m, 0.25 mm, 0.25 μm) and a flame ionization detector. Compounds were quantified by comparing the integrated peak areas of the compounds to external standard solutions. Precision of compound quantification is about 5% and precision of $U_{37}^{k'}$ reconstructions is 0.38°C based on multiple standard analyses. Compound-specific isotope analyses was carried out on a ThermoFisher Scientific MAT 253 Isotope Ratio Mass Spectrometer coupled via a GC Isolink operated at 1420°C to a ThermoFisher Scientific Trace GC equipped with a HP-5ms column (30 m, 0.25 mm, 1 μm). For each sample duplicate injections of C_{37} and palmitic acid were conducted. Measurement accuracy was controlled by *n*-alkane standards of known isotopic composition every six measurements and by the daily determination of the H_3^+ factor using H_2 as reference gas. H_3^+ factors varied between 5.6 and 6.2, while the mean absolute deviation of external standards was 2.2‰. In order to prevent a bias introduced by variable alkenone distribution, the δD of alkenones was analyzed for $C_{37:2}$ and $C_{37:3}$ together rather than separately (van der Meer et al., 2013). δD values for palmitic acid were corrected for the methyl group added during methylation.

3 Results

Onboard sea surface temperature measurements resulted in uniform values of 28.5 ± 0.5 °C, while salinity varied between 10 and 36 psu (Fig. 1; Table 1). The hydrogen isotope analyses of seawater samples yielded δD values between 6 and -15 ‰ (all isotope values are given vs.

VSMOW). The values correlated linearly with sea surface salinity (Fig. 2a). The suspended particle samples yielded C_{37} alkenone concentrations between 0.2-65.3 ng L^{-1} (Table 1). Samples with a salinity >25 psu showed variable concentrations (0.2-65.3 ng L^{-1}), while samples with a salinity <25 psu had concentrations consistently lower than 10 ng L^{-1}. There were little to no alkenones (concentration <1 ng L^{-1}) in filter samples with a salinity <15 psu (Fig. 2c, Table 1). The fatty acid analysis yielded almost exclusively short chain compounds, of which palmitic acid had concentrations between 1.4 and 27 μg L^{-1} (Fig. 2d). Variations in palmitic acid concentrations showed a weak inverse correlation with salinity (Fig. 2d). For samples with alkenone concentrations >10 ng L^{-1}, sea surface temperature reconstructions agreed within the calibration error of 1.5°C with onboard temperature measurements (Fig. 2b, Table 1). Samples with a concentration <10 ng L^{-1} featured a larger scatter with deviations from onboard measurements of up to 10°C (Fig. 2b). The ratio of the C_{37}/C_{38} alkenones resulted in values between 0.9 and 1.7 (Table 1), indicating the prevalence of open ocean haptophyte contribution throughout the transect (Rosell-Mele et al., 1994). The $C_{37:4}$ alkenone, sometimes used as a salinity proxy, was not present in our samples.

Due to the absence of alkenones in the low salinity samples, isotope analysis of the C_{37} alkenone was only possible in samples with a salinity > 15 psu. For these samples, δD_{C37} varied between -176 ‰ and -205 ‰ (Fig. 3a, Table 1). When all samples are taken into account, δD_{C37} and δD_{H_2O} do not correlate (Fig. 3a). If only the samples with an alkenone concentration >10 ng L^{-1} were considered, linear regression yielded a correlation between δD_{C37} and δD_{H2O} with a slope of 1.36 ‰ δD_{C37} per 1‰ δD_{H2O} ($r^2 = 0.51$, $p < 0.05$; Fig. 3a). $\alpha_{C_{37}}$ varied between 0.79 and 0.84 and showed no significant salinity dependence (Fig. 3c). In contrast to δD_{C37}, δD_{PA} strongly correlates with δD_{H_2O}, regardless of lipid concentration ($r^2 = 0.81$, $p < 10^{-7}$; Fig. 3b). The slope of the linear regression is 1.72 ‰ δD_{PA} per 1 ‰ $\delta D_{H2O.}$ The fractionation factor between palmitic acid and water (α_{PA}) yielded values between 0.79 and 0.83, featuring a significant salinity dependency with an increase of 0.001 per salinity unit (Fig. 3d).

4 Discussion

4.1 Lipid sources

4.1.1 Alkenone sources

The C_{37}/C_{38} ratio was used for the assessment of the dominant alkenone source (Conte et al., 1998). Open marine species like *Emiliana huxleyi* and *Gephyrocapsa oceanica* produce alkenones with a C_{37}/C_{38} between 0.5 and 1.5 (Conte et al., 1998). Coastal species like *Isochrysis galbana* and *Chrysotila lamellosa* produce alkenones with a C_{37}/C_{38} ratio >2, sometimes even >10 (M'Boule et al., 2014;Prahl et al., 1988;Marlowe et al., 1984). The C_{37}/C_{38} ratio of the samples from the Amazon Plume varied between 0.9 and 1.7 and alkenone production was therefore likely dominated by open marine species (Conte et al., 1998). Since some of the samples feature values at the upper limit for open marine species, some (probably small) contribution by coastal haptophytes cannot be ruled out (Kasper et al., 2015). Alternatively, the small variations in the C_{37}/C_{38} ratio could also be the effect of species variability within open marine haptophytes (Conte et al., 1998). In contrast to previous laboratory and field studies (Ono et al., 2009;Chu et al., 2005), we do not find a correlation between salinity and the C_{37}/C_{38} ratio (not shown here).

4.1.2 Palmitic acid sources

Palmitic acids are not exclusively produced by aqueous organisms and are also synthesized by terrestrial plants and bacteria (Eglinton and Eglinton, 2008). Unlike aqueous organisms, terrestrial plants also synthesize long-chain fatty acids (Eglinton and Hamilton, 1967), which were not present in the filter samples. This indicates that the palmitic acids found in the Amazon Plume are exclusively produced by aquatic organisms. Also, the fast turnover rates of palmitic acid makes a contribution by riverine compounds unlikely. Furthermore, previous studies have generally confirmed that palmitic acids in marine environments are predominantly produced by marine algae (Pearson et al., 2001).

4.2 Temperature reconstruction

Oceanic temperature reconstructions based on alkenones are a widely used tool in paleoclimatology (Bard et al., 1997;Rühlemann et al., 1999). The global calibrations in use are based on open marine haptophyte species (Prahl and Wakeham, 1987;Müller et al., 1998).

Our reconstructed temperatures show deviations of up to 10°C from instrumentally measured temperature for samples with alkenone concentration <10 ng L^{-1} (Fig. 2b). These anomalous, generally lower than expected values, could be caused by different processes. First, coastal species bear a temperature-$U_{37}^{k'}$ relationship with a markedly lower slope than open marine species (Sun et al., 2007;Versteegh et al., 2001). Hence, a larger alkenone contribution by coastal haptophyte species would lead to the observed lower temperatures. Second, lower salinity is reported to cause metabolic stress in alkenone producers leading to anomalous reconstructed temperatures (Harada et al., 2003). Third, variations in haptophyte growth rate due to nutrient or light limitation could also lead to variations in reconstructed temperatures (Epstein et al., 1998;Versteegh et al., 2001). The latter two points would also lead to lower alkenone concentrations and thus enhance the possibility of overprint by advection of allochthonous alkenones.

Variations in haptophyte algae composition recorded by changes in the C_{37}/C_{38} ratio do not show a correlation with the residue

$$T_{residue} = T_{measured} - T_{reconstructed} \quad (3)$$

of the temperature reconstruction (not shown here). Hence, variations in species composition are likely insufficient to account for the $T_{residue}$. Conversely, there is a correlation between $T_{residue}$ and salinity (Fig. 4a). Salinity might therefore be an important cause for the large $T_{residue}$ (Harada et al., 2003). The riverine waters of the Amazon Plume are generally nutrient rich (Santos et al., 2008), which makes a scenario of nutrient limitation unlikely to impact temperature control of $U_{37}^{k'}$ in our study area. The high sediment load delivered by the Amazon River, however, leads to light limitation in the study area (Smith and Demaster, 1996). Light limitation is indeed reported to lower reconstructed $U_{37}^{k'}$ temperatures by up to 7°C (Versteegh et al., 2001). Since diminished alkenone production due to low salinity and light limitation would lead to smaller alkenone concentrations, this would also explain why high concentration samples feature no temperature deviation (Fig. 4b). The advection of allochthonous alkenones biasing temperature reconstructions has been suggested in other studies (Rühlemann and Butzin, 2006;Benthien and Müller, 2000). In our samples, $U_{37}^{k'}$ overprint by advected alkenones can be considered less likely, since there are no nearby areas where alkenones with a lower temperature signal could originate from.

In conclusion, there are multiple potential factors influencing the $U_{37}^{k'}$ deviation in the Amazon Plume. Given that low alkenone concentrations are consistently associated with large negative temperature deviations, reduced alkenone production due to low salinity and light limitation in the Amazon Plume might be the most important factor for the temperature deviations (Fig. 4a, b) (Versteegh et al., 2001;Harada et al., 2003).

4.3 Stable hydrogen isotope signals

4.3.1 Alkenone δD

If all samples are considered, there is no correlation between δD_{C37} and δD_{H_2O} (Fig. 3a). Given the relationship between C_{37} concentration, $T_{residue}$ and salinity (Fig. 4a, b), we also tested whether there would be a better fit between δD_{C37} and δD_{H_2O} for high C_{37} concentration samples. There is indeed a correlation between δD_{C37} and δD_{H2O} for samples with a C_{37} concentration >10 ng L^{-1} (Fig. 3a). However, with a p-value of 0.05 and a low sample number of n=8, this relationship has to be viewed with caution. Nevertheless, we consider it to be an important information to study the potential factors leading to the deviation between δD_{C37} and δD_{H_2O}. Especially, since this relation reflects a generally constant α_{C37} of 0.81 and agrees with results obtained for open marine species cultured at different salinities (M'Boule et al., 2014). For a potential impact on δD_{C37}, factors similar to those considered for the temperature deviations have to be scrutinized: synthesis by coastal haptophyte species (M'Boule et al., 2014), changes in growth rate and phase (Schouten et al., 2006;Wolhowe et al., 2009), overprint by advected material and variations in salinity (Schouten et al., 2006). Since temperature is more or less uniform over the entire study area, a temperature effect as reported by Zhang and Sachs (2007) is not expected to play a role.

As previously mentioned, variations in the C_{37}/C_{38} ratio imply only limited variation in haptophyte species composition. Moreover, the values of α_{C37} are between 0.795 and 0.835 and are only slightly higher than observed in laboratory experiments studying open marine haptophytes (Schouten et al., 2006), but are markedly lower than observed for coastal haptophytes (M'Boule et al., 2014). This again suggests that the studied alkenones are predominantly of open marine haptophyte origin. Although there are no signs for a full scale change from open marine to coastal haptophytes, the variability in habitat preference may still be sufficient to have a significant influence on α_{C37}. The C_{37}/C_{38} variability found in a

sediment core collected offshore Mozambique by Kasper et al. (2015) was similar to the one found in our samples and the associated species variability was likely large enough to significantly influence δD_{C37}. In our samples, the C_{37}/C_{38} ratio does however not correlate with α_{C37} and species variations alone are therefore unlikely to be the dominant cause for the absent correlation between δD_{C37} and δD_{H2O} in low salinity samples. In contrast to laboratory studies (Schouten et al., 2006), we find no clear relationship between salinity and fractionation factor (Fig. 3c). The absence of a salinity-α_{C37} relationship was also reported in a field study by Schwab and Sachs (2011) who explained their findings by the presence of additional factors such as species variability and temperature, which may have counteracted the effects of salinity. If the relation between δD_{C37} and δD_{H2O} for high concentration samples is used to calculate the residue for each sample,

$$\delta D_{res\ C37} = \delta D_{C37} - \left(1.358 \times \delta D_{H_2O} - 194.558\right) \quad (4)$$

it becomes apparent that low concentration samples have higher residuals (Fig. 4d). Furthermore, $\delta D_{res\ C37}$ correlates with salinity, which indicates that $\delta D_{res\ C37}$ is largely influenced by the input of low salinity Amazon freshwater (Fig. 4c). This observation would also fit with the assumption that the lower C_{37} concentration in those samples were a result of lower growth rate, because lower growth rate leads to a higher fractionation factor (M'Boule et al., 2014;Schouten et al., 2006;Sachse and Sachs, 2008). Since the steep salinity gradient of the Amazon Plume leads to a wide range of surface water isotopic composition over a short geographic distance, we cannot exclude some influence of advected alkenones in samples with low or absent in situ alkenone production. As this effect is insufficient to explain the large $T_{residue}$, advection is likely not the main factor responsible for the absence of a correlation between δD_{C37} and δD_{H_2O}. Although the deviation in δD_{C37} cannot be tied to a single factor, low alkenone production associated with the low salinity, suspension rich Amazon waters is likely the most important factor (Wolhowe et al., 2015). Thus, the temperature- and δD_{C37} deviations are likely caused by similar effects (Fig. 4a-d).

4.3.2 Palmitic acid δD

In contrast to δD_{C37}, δD_{PA} correlates well with δD_{H2O} (Fig. 3b). Furthermore, α_{PA} correlates with salinity (Fig. 3d) and thus confirms the relationship between salinity and α observed in various laboratory and field studies for palmitic acid and other lipids (Schouten et al., 2006;M'Boule et al., 2014;Chivall et al., 2014a). Our findings imply that the limiting factors

potentially leading to variations in α_{C37} do not influence α_{PA}. The factors that could potentially influence δD_{PA} are largely similar to those influencing δD_{C37} (Chivall et al., 2014a). Unlike for alkenones there is, however, no clear evidence for a growth rate dependence of α_{PA} (Zhang et al. 2009).

One striking difference between palmitic acid and alkenones in our samples is the different abundance of the two compounds. Palmitic acid concentrations were about three orders of magnitude higher than alkenone concentrations (Fig. 2c, d). This is unsurprising, since palmitic acid is typically very abundant in marine environments (Pearson et al., 2001). In further contrast to the C_{37} concentration, the palmitic acid concentration was not lower in low salinity samples, but featured a trend towards higher concentrations. This indicates that palmitic acid producing organisms were not negatively affected by the low salinity, sediment rich Amazon input like haptophyte algae, but rather benefited from the high nutrient supply by the Amazon (Santos et al., 2008). This marked difference supports the notion that low alkenone production rates in parts of the study area were responsible for the α_{C37} deviations. Furthermore, the high palmitic acid concentrations also limit the influence of a possible overprint of the in situ signal by allochthonous compounds. Apart from that, the high turnover rate of palmitic acid may further impede the influence of allochthonous compounds. This is also in contrast to alkenones, which are comparably stable towards degradation (Sun and Wakeham 1994). Therefore, the lower turnover rate of alkenones renders these compounds more susceptible to overprint by older, allochthonous compounds.

Our study shows that α_{PA} remains relatively stable over a range of varying environmental conditions. This finding is similar to one reached by studies along a lake transect from Southern Canada to Florida, which found a good agreement between δD_{PA} and δD_{H2O} over a variety of ecological environments (Huang et al., 2004, 2002). The α_{PA} of 0.82 observed in those studies is also in the range of α_{PA} observed in the Amazon Plume (0.79-0.83). This further indicates that species composition and other factors are not influencing α_{PA} to a large extent on an ecosystem level. Potential variations of α_{PA} from different contributors are either small or levelled out by integration over ecosystems. A surprising constancy in δD_{PA} has also been observed in a sediment core from the Santa Barbara Basin (Li et al., 2009). There, the δD_{PA} remained constant even in the presence of heterotrophic palmitic acid producers. This could indicate that the constancy in α_{PA} is not only limited to phototrophic organisms as observed here and by Huang et al. (2004), but also extends to heterotrophic organisms. The

constancy could be caused by the very similar biosynthetic pathway for palmitic acid in bacteria and eukaryotes (Li et al., 2009).

Although there are multiple lacustrine studies successfully applying δD_{PA} as paleoenvironmental proxy (Smittenberg et al., 2011;Shuman et al., 2006) and δD_{PA} faithfully records δD_{H2O} in our study, there are still multiple factors that could overprint a surface δD_{PA} signal. Especially in open oceanic environments, palmitic acid production deeper in the water column could alter the signal recorded at the surface. After deposition, bacterial activity in the sediment could also overprint the original upper water column signal (Perry et al., 1979).

5 Conclusions

Our study shows that δD_{PA} in suspended particle samples from the Amazon Plume salinity gradient records variations in salinity. For δD_{C37}, this correlation is only present in samples above a C_{37} concentration of 10 ng L^{-1}. The low alkenone concentrations are likely caused by the sediment-rich freshwater input of the Amazon River impeding haptophyte growth and affecting α_{C37}. Hence, the ubiquitous nature of palmitic acid proved to be highly beneficial in the study area. Moreover, palmitic acid bears the advantage of easier isotopic measurement and a high availability in most environments. The use of δD_{PA} as a standalone salinity proxy has to be considered with caution. Potential disadvantages of palmitic acid include post depositional degradation, compound synthesis deeper in the water column, which may not record surface conditions and the bacterial overprint in the sediment. A possible way to circumvent these limitations, as well as the problems encountered for δD_{C37}, could be the alongside use of δD_{PA} and δD_{37}. δD_{PA} is not sensitive to the low concentration issues encountered in this study, while δD_{C37} is only produced in surface waters and not susceptible to synthesis or degradation deeper in the water column or sediments. Therefore, the combined study of compound-specific hydrogen isotope composition of more than one compound could yield important information on influences in δD_{Lipid} other than salinity.

Acknowledgements

We would like to acknowledge funding through the DFG-Research Center / Cluster of Excellence „The Ocean in the Earth System“ at MARUM- Center for Environmental Sciences. CH thanks GLOMAR – Bremen International Graduate School for Marine Sciences for support and CMC acknowledges financial support from FAPESP (grant 2012/17517-3). We thank the *RV Maria S. Merian* cruise MSM20/3 crew for technical support during sampling, and Ralph Kreutz and Ana C. R. de Albergaria-Barbosa for laboratory support.

References

Bard, E., Rostek, F., and Sonzogni, C.: Interhemispheric synchrony of the last deglaciation inferred from alkenone palaeothermometry, Nature, 385, 707-710, 10.1038/385707a0, 1997.

Benthien, A., and Müller, P. J.: Anomalously low alkenone temperatures caused by lateral particle and sediment transport in the Malvinas Current region, western Argentine Basin, Deep-Sea Res. Part I-Oceanogr. Res. Pap., 47, 2369-2393, 10.1016/s0967-0637(00)00030-3, 2000.

Chivall, D., M'Boule, D., Heinzelmann, S. M., Kasper, S., Sinke-Schoen, D., Sinninghe-Damsté, J. S., Schouten, S., and van der Meer, M. T. J.: Towards a palaeosalinity proxy: hydrogen isotopic fractionation between source water and lipids produced via different biosynthetic pathways in haptophyte algae, Geophysical Research Abstracts, 16, 12066, 2014a.

Chivall, D., M'Boule, D., Sinke-Schoen, D., Sinninghe Damsté, J. S., Schouten, S., and van der Meer, M. T. J.: The effects of growth phase and salinity on the hydrogen isotopic composition of alkenones produced by coastal haptophyte algae, Geochim. Cosmochim. Acta, 140, 381-390, 10.1016/j.gca.2014.05.043, 2014b.

Chu, G. Q., Sun, Q., Li, S. Q., Zheng, M. P., Jia, X. X., Lu, C. F., Liu, J. Q., and Liu, T. S.: Long-chain alkenone distributions and temperature dependence in lacustrine surface sediments from China, Geochim. Cosmochim. Acta, 69, 4985-5003, 10.1016/j.gca.2005.04.008, 2005.

Conte, M. H., Thompson, A., Lesley, D., and Harris, R. P.: Genetic and physiological influences on the alkenone/alkenoate versus growth temperature relationship in Emiliania huxleyi and Gephyrocapsa oceanica, Geochim. Cosmochim. Acta, 62, 51-68, 10.1016/s0016-7037(97)00327-x, 1998.

Eglinton, G., and Hamilton, R. J.: Leaf epicuticular waxes, Science, 156, 1322-1335, 10.1126/science.156.3780.1322, 1967.

Eglinton, T. I., and Eglinton, G.: Molecular proxies for paleoclimatology, Earth Planet. Sci. Lett., 275, 1-16, 10.1016/j.epsl.2008.07.012, 2008.

Englebrecht, A. C., and Sachs, J. P.: Determination of sediment provenance at drift sites using hydrogen isotopes and unsaturation ratios in alkenones, Geochim. Cosmochim. Acta, 69, 4253-4265, 10.1016/j.gca.2005.04.011, 2005.

Epstein, B. L., D'Hondt, S., Quinn, J. G., Zhang, J. P., and Hargraves, P. E.: An effect of dissolved nutrient concentrations on alkenone-based temperature estimates, Paleoceanography, 13, 122-126, 10.1029/97pa03358, 1998.

Epstein, S., and Mayeda, T.: Variation of O18 content of waters from natural sources, Geochim. Cosmochim. Acta, 4, 213-224, 10.1016/0016-7037(53)90051-9, 1953.

Geyer, W. R., Beardsley, R. C., Lentz, S. J., Candela, J., Limeburner, R., Johns, W. E., Castro, B. M., and Soares, I. D.: Physical oceanography of the Amazon shelf, Cont. Shelf Res., 16, 575-616, 10.1016/0278-4343(95)00051-8, 1996.

Giosan, L., Coolen, M. J. L., Kaplan, J. O., Constantinescu, S., Filip, F., Filipova-Marinova, M., Kettner, A. J., and Thom, N.: Early Anthropogenic Transformation of the Danube-Black Sea System, Sci. Rep., 2, 10.1038/srep00582, 2012.

Harada, N., Shin, K. H., Murata, A., Uchida, M., and Nakatani, T.: Characteristics of alkenones synthesized by a bloom of Emiliania huxleyi in the Bering Sea, Geochim. Cosmochim. Acta, 67, 1507-1519, 10.1016/s0016-7037(02)01318-2, 2003.

Huang, Y. S., Shuman, B., Wang, Y., and Webb, T.: Hydrogen isotope ratios of palmitic acid in lacustrine sediments record late Quaternary climate variations, Geology, 30, 1103-1106, 10.1130/0091-7613(2002)030<1103:hiropa>2.0.co;2, 2002.

Huang, Y. S., Shuman, B., Wang, Y., and Webb, T.: Hydrogen isotope ratios of individual lipids in lake sediments as novel tracers of climatic and environmental change: a surface sediment test, J. Paleolimn., 31, 363-375, 10.1023/b:jopl.0000021855.80535.13, 2004.

Kasper, S., van der Meer, M. T. J., Castañeda, I. S., Tjallingii, R., Brummer, G.-J. A., Sinninghe Damsté, J. S., and Schouten, S.: Testing the alkenone D/H ratio as a paleo indicator of sea surface salinity in a coastal ocean margin (Mozambique Channel), Org Geochem, 78, 62-68, 10.1016/j.orggeochem.2014.10.011, 2015.

Lea, D. W., Pak, D. K., and Spero, H. J.: Climate impact of late Quaternary equatorial Pacific sea surface temperature variations, Science, 289, 1719-1724, 10.1126/science.289.5485.1719, 2000.

Lentz, S. J., and Limeburner, R.: The Amazon River Plume during AMASSEDS - Spatial characteristics and salinity variability, J. Geophys. Res.-Oceans, 100, 2355-2375, 10.1029/94jc01411, 1995.

Li, C., Sessions, A. L., Kinnaman, F. S., and Valentine, D. L.: Hydrogen-isotopic variability in lipids from Santa Barbara Basin sediments, Geochim. Cosmochim. Acta, 73, 4803-4823, 10.1016/j.gca.2009.05.056, 2009.

M'Boule, D., Chivall, D., Sinke-Schoen, D., Sinninghe-Damsté, J. S., Schouten, S., and van der Meer, M. T. J.: Salinity dependent hydrogen isotope fractionation in alkenones produced by coastal and open ocean haptophyte algae, Geochim. Cosmochim. Acta, 130, 126-135, 10.1016/j.gca.2014.01.029, 2014.

Marlowe, I. T., Green, J. C., Neal, A. C., Brassell, S. C., Eglinton, G., and Course, P. A.: Long-Chain (n-C37-C39) Alkenones in the Prymnesiophyceae - Distribution of Alkenones and other Lipids and their Taxonomic Significance, British Phycological Journal, 19, 203-216, 1984.

Marlowe, I. T., Brassell, S. C., Eglinton, G., and Green, J. C.: Long-Chain Alkenones and Alkyl Alkenoates and the Fossil Coccolith Record of Marine Sediments, Chemical Geology, 88, 349-375, 10.1016/0009-2541(90)90098-r, 1990.

Molleri, G. S. F., Novo, E., and Kampel, M.: Space-time variability of the Amazon River plume based on satellite ocean color, Cont. Shelf Res., 30, 342-352, 10.1016/j.csr.2009.11.015, 2010.

Mulitza, S., Chiessi, C. M., Cruz, A. P. S., Frederichs, T., Gomes, J. G., Gurgel, M. H., Haberkern, J., Huang, E., Jovane, L., Kuhnert, H., Pittauerová, D., Reiners, S.-J., Roud, S. C., Schefuß, E., Schewe, F., Schwenk, T. A., Sicoli Seoane, J. C., Sousa, S. H. M., Wagner, D. J., and Wiers, S.: Response of Amazon sedimentation to deforestation, land use and climate variability – Cruise No. MSM20/3 - February 19 - March 11, 2012 - Recife (Brazil) - Bridgetown (Barbados), Berichte, Fachbereich Geowissenschaften, Universität Bremen, Bremen, Germany, 1-86, 2013.

Müller, P. J., Kirst, G., Ruhland, G., von Storch, I., and Rosell-Mele, A.: Calibration of the alkenone paleotemperature index U-37(K ') based on core-tops from the eastern South Atlantic and the global ocean (60 degrees N-60 degrees S), Geochim. Cosmochim. Acta, 62, 1757-1772, 10.1016/s0016-7037(98)00097-0, 1998.

Nelson, D. B., and Sachs, J. P.: The influence of salinity on D/H fractionation in dinosterol and brassicasterol from globally distributed saline and hypersaline lakes, Geochim. Cosmochim. Acta, 133, 325-339, 10.1016/j.gca.2014.03.007, 2014.

Ono, M., Sawada, K., Kubota, M., and Shiraiwa, Y.: Change of the unsaturation degree of alkenone and alkenoate during acclimation to salinity change in Emiliania huxleyi and Gephyrocapsa oceanica with reference to palaeosalinity indicator., Res. Org. Geochem, 25, 53-60, 2009.

Pahnke, K., Sachs, J. P., Keigwin, L., Timmermann, A., and Xie, S. P.: Eastern tropical Pacific hydrologic changes during the past 27,000 years from D/H ratios in alkenones, Paleoceanography, 22, 15, 10.1029/2007pa001468, 2007.

Pearson, A., McNichol, A. P., Benitez-Nelson, B. C., Hayes, J. M., and Eglinton, T. I.: Origins of lipid biomarkers in Santa Monica Basin surface sediment: A case study using compound-specific Delta C-14 analysis, Geochim. Cosmochim. Acta, 65, 3123-3137, 10.1016/s0016-7037(01)00657-3, 2001.

Perry, G. J., Volkman, J. K., Johns, R. B., and Bavor Jr, H. J.: Fatty acids of bacterial origin in contemporary marine sediments, Geochim. Cosmochim. Acta, 43, 1715-1725, 10.1016/0016-7037(79)90020-6, 1979.

Prahl, F. G., and Wakeham, S. G.: Calibration of unsaturation patterns in long-chain ketone compositions or paleotemperature assessment, Nature, 330, 367-369, 10.1038/330367a0, 1987.

Prahl, F. G., Muehlhausen, L. A., and Zahnle, D. L.: Further Evalutation of Long-Chain Alkenones as Indicators of Paleoceanographic Conditions, Geochim. Cosmochim. Acta, 52, 2303-2310, 10.1016/0016-7037(88)90132-9, 1988.

Rohling, E. J.: Progress in paleosalinity: Overview and presentation of a new approach, Paleoceanography, 22, PA3215, 10.1029/2007pa001437, 2007.

Rosell-Mele, A., Carter, J., and Eglinton, G.: Distributions of long-chain alkenones and alkyl alkenoates in marine surface sediments from the North-East Atlantic, Org Geochem, 22, 501-509, 10.1016/0146-6380(94)90122-8, 1994.

Rostek, F., Ruhland, G., Bassinot, F. C., Muller, P. J., Labeyrie, L. D., Lancelot, Y., and Bard, E.: Reconstructing Sea-Surface Temperature and Salinity using Delta-O-18 and Alkenone Records, Nature, 364, 319-321, 10.1038/364319a0, 1993.

Rühlemann, C., Mulitza, S., Muller, P. J., Wefer, G., and Zahn, R.: Warming of the tropical Atlantic Ocean and slowdown of thermohaline circulation during the last deglaciation, Nature, 402, 511-514, 10.1038/990069, 1999.

Rühlemann, C., and Butzin, M.: Alkenone temperature anomalies in the Brazil-Malvinas Confluence area caused by lateral advection of suspended particulate material, Geochem. Geophys. Geosyst., 7, Q10015, 10.1029/2006gc001251, 2006.

Sachse, D., and Sachs, J. P.: Inverse relationship between D/H fractionation in cyanobacterial lipids and salinity in Christmas Island saline ponds, Geochim. Cosmochim. Acta, 72, 793-806, 10.1016/j.gca.2007.11.022, 2008.

Santos, M. L. S., Muniz, K., Barros-Neto, B., and Araujo, M.: Nutrient and phytoplankton biomass in the Amazon River shelf waters, An. Acad. Bras. Cienc., 80, 703-717, 10.1590/s0001-37652008000400011, 2008.

Sauer, P. E., Eglinton, T. I., Hayes, J. M., Schimmelmann, A., and Sessions, A. L.: Compound-specific D/H ratios of lipid biomarkers from sediments as a proxy for environmental and climatic conditions, Geochim. Cosmochim. Acta, 65, 213-222, 10.1016/s0016-7037(00)00520-2, 2001.

Schmidt, F., Oberhansli, H., and Wilkes, H.: Biocoenosis response to hydrological variability in Southern Africa during the last 84 ka BP: A study of lipid biomarkers and compound-specific stable carbon and hydrogen isotopes from the hypersaline Lake Tswaing, Glob. Planet. Change, 112, 92-104, 10.1016/j.gloplacha.2013.11.004, 2014.

Schouten, S., Ossebaar, J., Schreiber, K., Kienhuis, M. V. M., Langer, G., Benthien, A., and Bijma, J.: The effect of temperature, salinity and growth rate on the stable hydrogen isotopic composition of long chain alkenones produced by Emiliania huxleyi and Gephyrocapsa oceanica, Biogeosciences, 3, 113-119, 10.5194/bg-3-113-2006, 2006.

Schwab, V. F., and Sachs, J. P.: The measurement of D/H ratio in alkenones and their isotopic heterogeneity, Org Geochem, 40, 111-118, 10.1016/j.orggeochem.2008.09.013, 2009.

Schwab, V. F., and Sachs, J. P.: Hydrogen isotopes in individual alkenones from the Chesapeake Bay estuary, Geochim. Cosmochim. Acta, 75, 7552-7565, 10.1016/j.gca.2011.09.031, 2011.

Sessions, A. L., Burgoyne, T. W., Schimmelmann, A., and Hayes, J. M.: Fractionation of hydrogen isotopes in lipid biosynthesis, Org Geochem, 30, 1193-1200, 10.1016/s0146-6380(99)00094-7, 1999.

Shuman, B., Huang, Y. S., Newby, P., and Wang, Y.: Compound-specific isotopic analyses track changes in seasonal precipitation regimes in the Northeastern United States at ca 8200cal yrBP, Quat. Sci. Rev., 25, 2992-3002, 10.1016/j.quascirev.2006.02.021, 2006.

Smith, W. O., and Demaster, D. J.: Phytoplankton biomass and productivity in the Amazon River plume: Correlation with seasonal river discharge, Cont. Shelf Res., 16, 291-319, 10.1016/0278-4343(95)00007-n, 1996.

Smittenberg, R. H., Saenger, C., Dawson, M. N., and Sachs, J. P.: Compound-specific D/H ratios of the marine lakes of Palau as proxies for West Pacific Warm Pool hydrologic variability, Quat. Sci. Rev., 30, 921-933, 10.1016/j.quascirev.2011.01.012, 2011.

Sun, M. Y., and Wakeham, S. G.: Molecular evidence for degradation and preservation of organic matter in the anoxic Black-Sea Basin, Geochim. Cosmochim. Acta, 58, 3395-3406, 10.1016/0016-7037(94)90094-9, 1994.

Sun, Q., Chu, G. Q., Liu, G. X., Li, S., and Wang, X. H.: Calibration of alkenone unsaturation index with growth temperature for a lacustrine species, Chrysotila lamellosa (Haptophyceae), Org Geochem, 38, 1226-1234, 10.1016/j.orggeochem.2007.04.007, 2007.

van der Meer, M. T. J., Baas, M., Rijpstra, W. I. C., Marino, G., Rohling, E. J., Sinninghe Damsté, J. S., and Schouten, S.: Hydrogen isotopic compositions of long-chain alkenones record freshwater flooding of the Eastern Mediterranean at the onset of sapropel deposition, Earth Planet. Sci. Lett., 262, 594-600, 10.1016/j.epsl.2007.08.014, 2007.

van der Meer, M. T. J., Sangiorgi, F., Baas, M., Brinkhuis, H., Sinninghe Damsté, J. S., and Schouten, S.: Molecular isotopic and dinoflagellate evidence for Late Holocene freshening of the Black Sea, Earth Planet. Sci. Lett., 267, 426-434, 10.1016/j.epsl.2007.12.001, 2008.

van der Meer, M. T. J., Benthien, A., Bijma, J., Schouten, S., and Sinninghe Damsté, J. S.: Alkenone distribution impacts the hydrogen isotopic composition of the C-37:2 and C-37:3 alkan-2-ones in Emiliania huxleyi, Geochim. Cosmochim. Acta, 111, 162-166, 10.1016/j.gca.2012.10.041, 2013.

Versteegh, G. J. M., Riegman, R., de Leeuw, J. W., and Jansen, J. H. F.: U(37)(K ')values for Isochrysis galbana as a function of culture temperature, light intensity and nutrient concentrations, Org Geochem, 32, 785-794, 10.1016/s0146-6380(01)00041-9, 2001.

Wolhowe, M. D., Prahl, F. G., Probert, I., and Maldonado, M.: Growth phase dependent hydrogen isotopic fractionation in alkenone-producing haptophytes, Biogeosciences, 6, 1681-1694, 10.5194/bg-6-1681-2009, 2009.

Wolhowe, M. D., Prahl, F. G., Langer, G., Oviedo, A. M., and Ziveri, P.: Alkenone δD as an ecological indicator: A culture and field study of physiologically-controlled chemical and hydrogen-isotopic variation in C37 alkenones, Geochim. Cosmochim. Acta, 162, 166-182, 10.1016/j.gca.2015.04.034, 2015.

Zhang, Z. H., and Sachs, J. P.: Hydrogen isotope fractionation in freshwater algae: I. Variations among lipids and species, Org Geochem, 38, 582-608, 10.1016/j.orggeochem.2006.12.004, 2007.

Zhang, Z. H., Sachs, J. P., and Marchetti, A.: Hydrogen isotope fractionation in freshwater and marine algae: II. Temperature and nitrogen limited growth rate effects, Org Geochem, 40, 428-439, 10.1016/j.orggeochem.2008.11.002, 2009.

Table 1. Average geographic position, average measured sea surface temperature (SST), average sea surface salinity (SSS), C_{37} concentration, palmitic acid (PA) concentration, $U^{k'}_{37}$, C_{37}/C_{38} ratio, δD of water (δD_{H_2O}), δD of C_{37} (δD_{C37}) and δD of palmitic acid (δD_{PA})for each sample. Values for salinity and temperature are the average of onboard measurements taken in one second intervals during each filtering period. Errors represent the standard deviation of these measurements. δD values of water represent the mean of two samples taken at the beginning and the end of each filtering period, each sample represents the mean of ten replicate injections. Errors represent the propagated standard deviation of these measurements. δD values of C_{37} and palmitic acid are the means of duplicate measurements. Errors represent the range between the duplicate measurements.

Sample	Lat.	Long.	SST (C°)	SSS (psu)	Conc. C_{37} (ng L^{-1})	Conc. PA (µg L^{-1})	$U^{k'}_{37}$	C_{37}/C_{38}	δD_{H_2O}	δD C_{37}	δD PA
PP10	1.9035	-48.4169	28.37 ± 0.03	36.2 ± 0.09	47.7	1.3	0.98	1.46	4.8 ± 0.9	-190.1 ± 0.5	-170.8 ± 1
PP11	1.7587	-48.2568	28.99 ± 0.04	34.72 ± 0.51	54.2	N/A	0.96	1.56	6.6 ± 1.2	-189.2 ± 3.7	N/A
PP12	1.7123	-48.2975	29.28 ± 0.05	31.65 ± 1.1	65.3	6	0.95	1.45	2.3 ± 1.1	-185.4 ± 2.2	-183.5 ± 0.8
PP13	1.6655	-48.3388	29.31 ± 0.18	28.06 ± 1.2	20.6	16.6	0.96	1.47	-2.6 ± 1.6	-200.8 ± 1.9	-193.2 ± 1.7
PP14	1.6197	-48.3791	29.17 ± 0.03	25.79 ± 0.51	5.7	12.3	0.94	1.42	-4.1 ± 1.1	-206.3 ± 1.3	-197.5 ± 0.4
PP15	1.5724	-48.421	29.28 ± 0.05	22.86 ± 0.47	8.6	19.4	0.95	1.44	-6.7 ± 1	a	-205.4 ± 0.9
PP16	1.5676	-48.4632	29.23 ± 0.05	20.91 ± 0.47	1.4	13.9	0.89	1.33	-9.2 ± 0.9	a	-209.7 ± 0.6
PP17	1.6199	-48.5119	29.02 ± 0.07	20.55 ± 0.41	1.5	8.7	0.89	1.19	-11.8 ± 1.4	-176.9 ± 0.3	-205.9 ± 0
PP19	2.0306	-48.759	28.67 ± 0.02	17.84 ± 0.55	3.8	N/A	0.71	2.52	-14.5 ± 1.3	a	N/A
PP20	2.0858	-48.7282	28.73 ± 0.03	21.15 ± 1.38	2.6	N/A	0.81	1.08	N/A	a	N/A
PP21	2.1431	-48.6728	28.82 ± 0.02	26.22 ± 1.63	1.3	N/A	0.79	1.12	N/A	a	N/A
PP22	2.1815	-48.6369	28.82 ± 0.05	30.76 ± 1.2	2.8	N/A	0.91	1.44	N/A	a	N/A
PP23	2.2205	-48.6038	28.9 ± 0.02	33.25 ± 0.5	2.8	N/A	0.95	1.43	N/A	a	N/A
PP24	2.259	-48.6055	28.93 ± 0.02	33.89 ± 0.11	4.9	N/A	0.97	0.99	3.8 ± 0.9	-191.8 ± 1.9	N/A
PP25	2.3389	-48.7336	28.84 ± 0.04	27.45 ± 1.27	5.1	N/A	0.87	0.92	N/A	a	N/A
PP26	2.2984	-48.7711	28.82 ± 0.03	23.96 ± 1.09	0.4	N/A	0.87	1.25	N/A	a	N/A
PP27	2.2674	-48.7995	28.71 ± 0.04	20.8 ± 0.71	0.4	N/A	0.65	0.98	N/A	a	N/A
PP33	2.0652	-48.5919	28.6 ± 0.04	17.44 ± 0.24	1.1	N/A	0.68	1.01	N/A	a	N/A
PP34	1.9301	-48.5528	28.63 ± 0.04	16.02 ± 0.12	6.6	N/A	0.78	1.27	N/A	a	N/A
PP35	1.7071	-48.4395	28.45 ± 0.04	18.21 ± 0.39	0.8	N/A	0.76	1.03	N/A	a	N/A
PP36	1.6196	-48.4013	28.55 ± 0.06	24.34 ± 0.4	2.2	16.5	0.85	1.17	-9.1 ± 1.2	a	-204.3 ± 0.2
PP37	1.7662	-48.4925	28.37 ± 0.03	17.63 ± 1.27	0.6	N/A	0.76	1.2	N/A	a	N/A
PP38	2.0088	-48.6108	28.35 ± 0.05	14.14 ± 0.76	0.7	N/A	0.64	1.02	-17.4 ± 0.9	a	N/A
PP40	2.8827	-49.4089	28.73 ± 0.03	33.54 ± 0.06	4.0	N/A	0.81	0.99	N/A	a	N/A
PP41	2.8566	-49.3425	29.08 ± 0.06	29.34 ± 1.32	0.2	2.1	0.81	1.8	0.2 ± 0.9	a	-188 ± 1.1
PP42	2.8342	-49.3151	29.04 ± 0.03	26.65 ± 1.52	0.2	2.0	0.86	1.25	-2.2 ± 1.1	a	-197.1 ± 0.7
PP43	3.1391	-49.3335	28.46 ± 0.04	36.16 ± 0.11	16.7	5.5	0.97	1.55	5.9 ± 1.3	-180.3 ± 0.6	-183.4 ± 0.8
PP44	3.0999	-49.3064	28.23 ± 0.03	34.89 ± 0.45	59.1	N/A	0.98	1.54	6.3 ± 1.1	-189 ± 1.4	N/A
PP45	3.0627	-49.4272	28.51 ± 0.02	32.83 ± 0.8	33.3	N/A	0.98	1.63	4.1 ± 0.9	-190.8 ± 0.4	N/A
PP46	3.0911	-49.4337	28.68 ± 0.04	33.1 ± 0.65	9.2	N/A	0.96	1.42	N/A	a	N/A
PP47	3.0554	-49.4321	28.49 ± 0.01	29.2 ± 0.08	6.1	16.4	0.96	1.29	0 ± 0.9	-177.2 ± 1.4	-201.6 ± 0.7
PP48	2.915	-49.3347	28.03 ± 0.02	23.42 ± 0.27	7.7	7.2	0.88	1.14	-9.2 ± 1.4	-197.9 ± 0.5	-202.3 ± 1.6
PP49	2.8972	-49.4713	28.07 ± 0.03	21.86 ± 0.46	1.3	16.2	0.89	1.23	-8.4 ± 1	a	-211.7 ± 0.3
PP51	3.1025	-49.7931	28.3 ± 0.06	18.31 ± 0.21	2.2	N/A	0.74	1.04	N/A	a	N/A
PP52	3.098	-49.6761	28.68 ± 0.03	24.91 ± 0.16	0.6	27.0	0.86	1.23	-10 ± 1.3	a	-204.9 ± 1.6
PP53	3.5031	-50.1667	28.25 ± 0.08	20.33 ± 1.93	1.0	N/A	0.85	1.38	N/A	a	N/A
PP54	3.5576	-50.3623	28.2 ± 0.1	18.63 ± 0.6	0.3	11.9	0.82	1.05	N/A	a	N/A
PP55	3.9688	-50.5373	28.27 ± 0.16	16.94 ± 1.38	0.7	N/A	0.75	1.04	-16 ± 0.8	a	N/A
PP57	4.4874	-51.2401	28.04 ± 0.05	15.88 ± 0.09	0.1	17.7	0.82	b	-18.2 ± 0.7	a	-220.3 ± 0.8
PP60	6.1499	-51.2679	28.09 ± 0.03	36.16 ± 0.01	2.0	2.7	0.99	b	5.8 ± 0.8	-183.2 ± 1.2	-182.4 ± 0.6
PP61	5.5698	-51.8561	27.93 ± 0.09	32.19 ± 1.28	23.4	N/A	0.98	1.11	2.1 ± 1.3	-191.1 ± 2.7	N/A
PP62	5.3201	-51.9255	27.9 ± 0.04	22.72 ± 1.32	3.4	23.2	0.97	1.1	-8.3 ± 0.9	-192 ± 5.4	-209.7 ± 1.4
PP65	4.766	-51.5166	27.55 ± 0.08	17.58 ± 4.51	1.1	20.2	0.97	1.05	N/A	a	N/A
PP66	6.658	-52.8391	28.09 ± 0	36.06 ± 0	7.1	4.01	0.96	1.2	6.2 ± 0.7	-195.5 ± 0.1	-188.9 ± 0.5
PP67	5.9423	-52.6319	27.91 ± 0.07	25.25 ± 1.1	9.2	13.4	0.97	1.32	-4.9 ± 1.2	-183.7 ± 2	-206.7 ± 0
PP68	5.79	-52.7484	27.53 ± 0.06	23.4 ± 0.17	4.6	N/A	0.96	1.16	-7.1 ± 1.2	-192.5 ± 0.4	N/A
PP69	6.0839	-53.601	27.47 ± 0.03	22.69 ± 0.24	2.5	N/A	0.8	1.45	N/A	a	N/A
PP70	6.2821	-53.1561	27.64 ± 0.03	24.96 ± 0.74	2.4	N/A	0.96	1.03	N/A	a	N/A

[N/A] No measurements conducted

[a] C_{37} yield was not high enough for isotope analysis

[b] No clear peak distinction for C_{38}

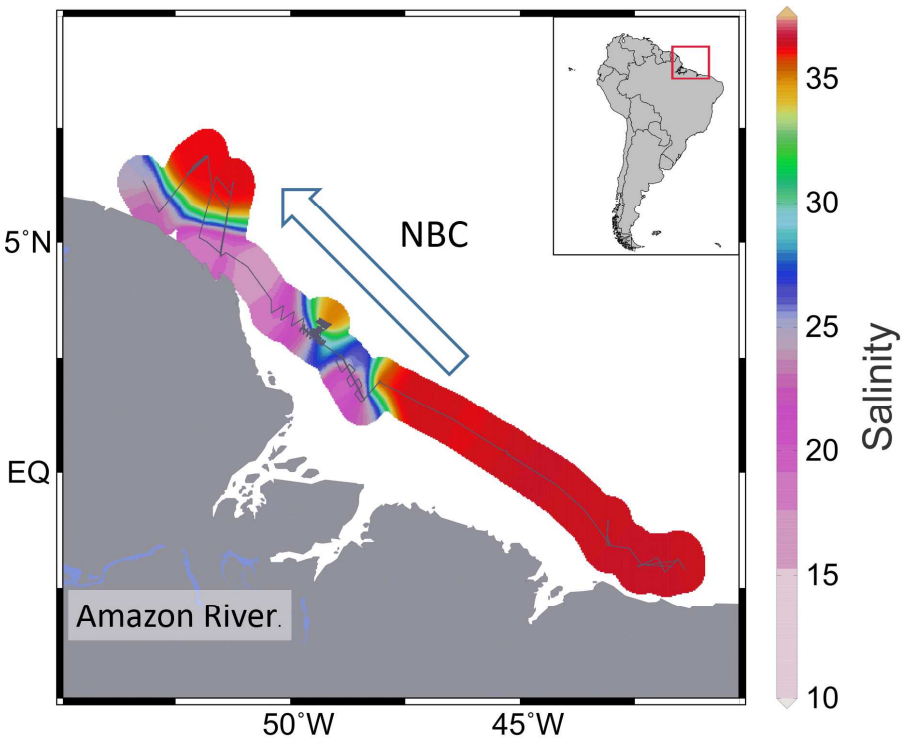

Figure 1. Map of the low salinity plume of the Amazon River outflow derived from the interpolation of onboard salinity measurements. The grey line shows RV Maria S. Merian cruise track MSM20/3 (Mulitza et al., 2013). The blue arrow depicts the North Brazil Current (NBC).

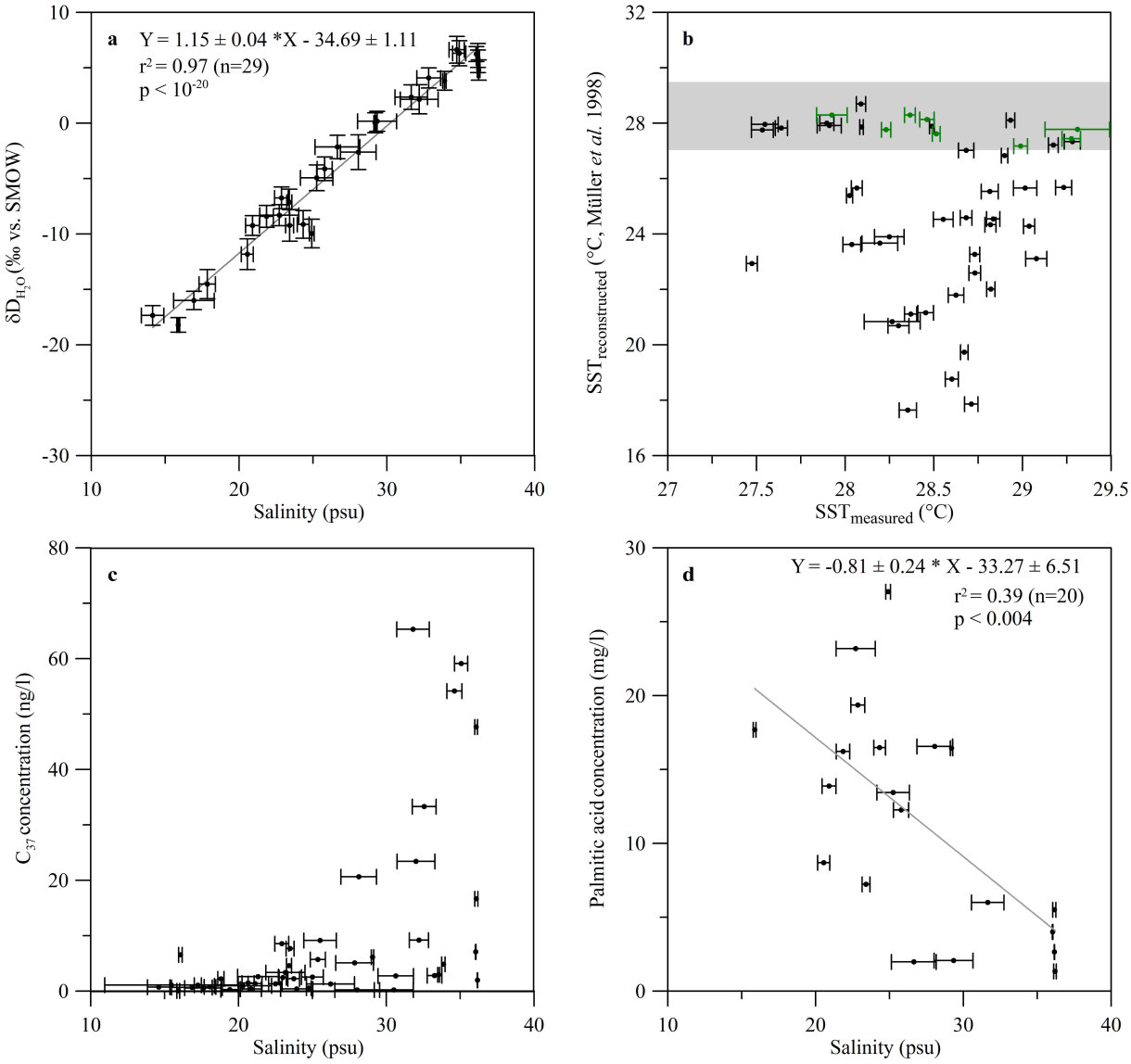

Figure 2. a) δD_{H_2O} plotted against salinity; b) $U_{37}^{k'}$ based sea surface temperature (SST) reconstruction using the calibration by Müller et al. (1998) plotted against measured temperature. Green data points represent samples with a C_{37} concentration > 10 ng L^{-1}. The grey bar indicates the range of measured SST; c) Concentration of the C_{37} alkenones plotted against salinity; d) Palmitic acid concentration plotted against salinity.

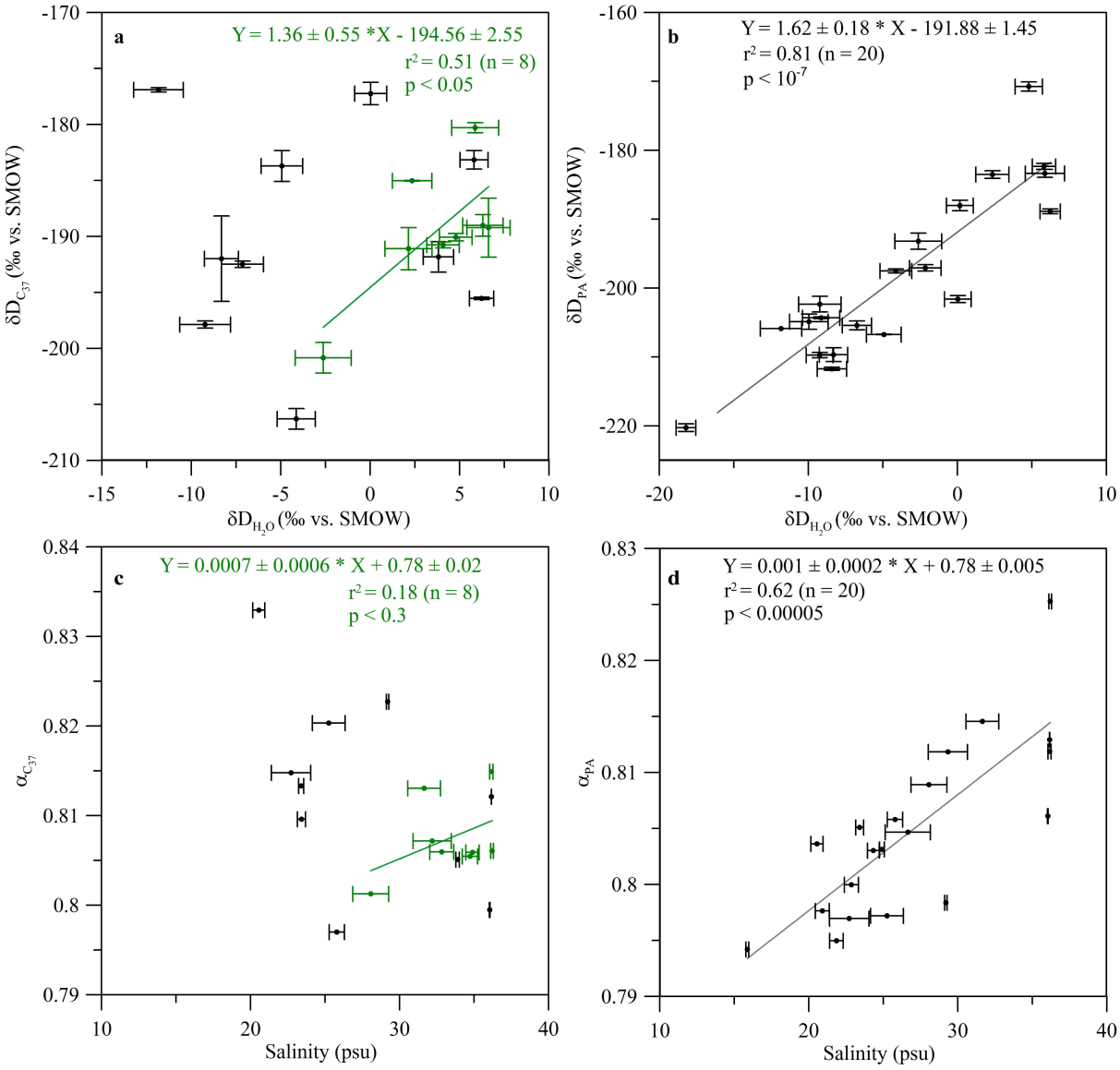

Figure 3. Results of the δD_{lipid} analysis. a) $\delta D_{C_{37}}$ against δD_{H_2O}. Green data points represent samples with a C_{37} concentration > 10 ng L^{-1}; b) δD_{PA} against δD_{H_2O}; c) $\alpha_{C_{37}}$ against salinity. Green data points represent samples with a C_{37} concentration > 10 ng L^{-1}; d) α_{PA} against salinity.

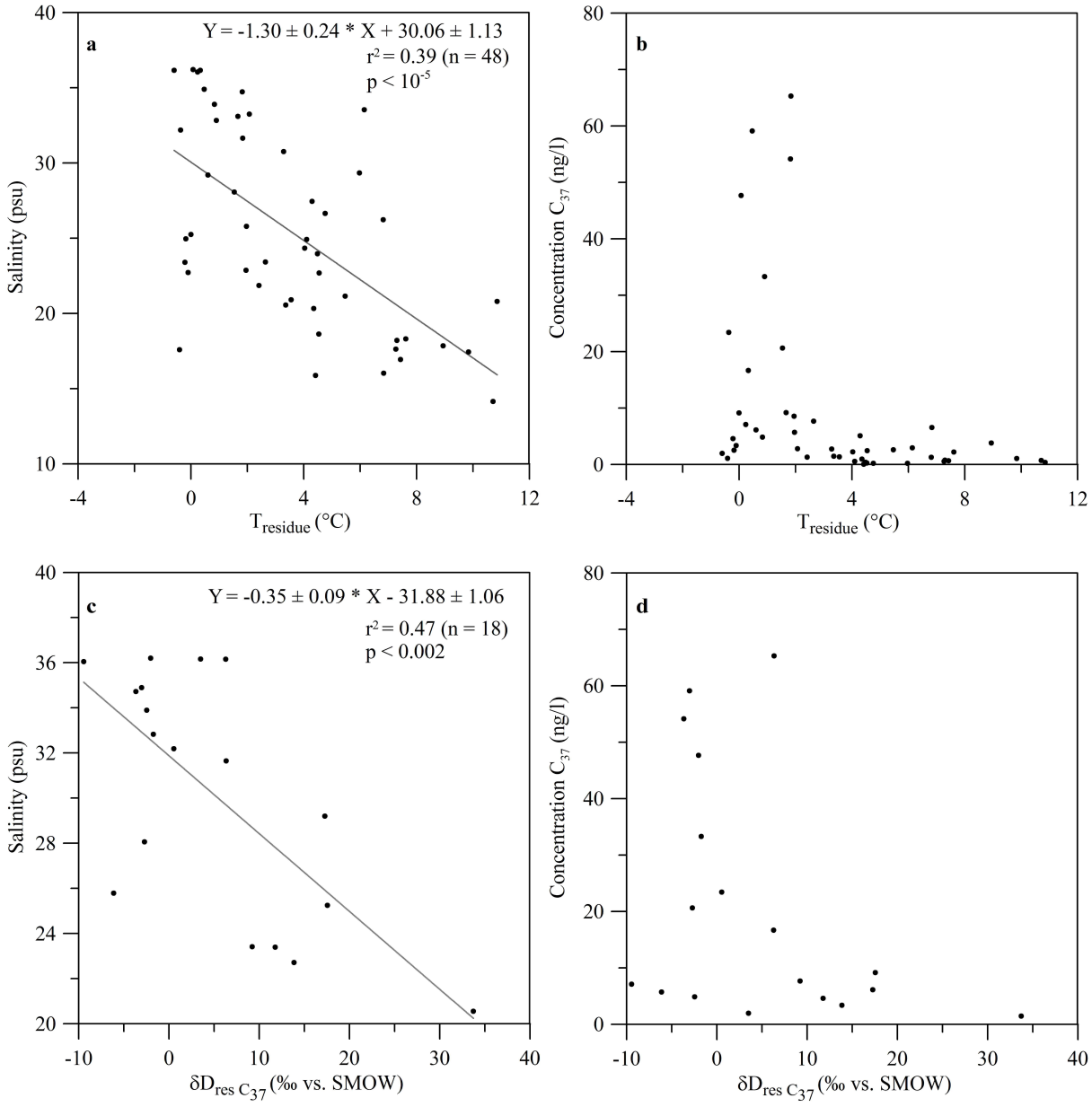

1

2 Figure 4. Residues of the $U_{37}^{k'}$ based SST reconstruction plotted against salinity (a) and C_{37}
3 concentration (b). Residues of the $\delta D_{C_{37}}$ measurement plotted against salinity (c) and C_{37}
4 concentration (d).